other aspects of theta pinches.[7-11] The observation of this delay in Scylla IV-P is therefore a strong indication of the presence of microturbulent heating in the post-implosion phase of this high-density experiment. This delay time is very sensitive to the additional heating, even though the total neutron yield is not. Because microturbulent transport in field-reversed theta pinches is a critical issue in the determination of the amount of trapped flux remaining after the formation of the configuration, such delays could be looked for in future field-reversed theta-pinch experiments, and may be viewed as a diagnostic of nonadiabatic plasma heating.

[a]Permanent address: Mission Research Corporation, 1400 San Mateo Blvd. SE, Albuquerque, N. Mex. 87108.

[b]Permanent address: JAYCOR, 205 S. Whiting St., Alexandria, Va. 22032.

[1]K. Boyer, W. C. Elmore, E. M. Little, W. E. Quinn, and J. L. Tuck, Phys. Rev. 119, 831 (1960).

[2]W. T. Armstrong, R. K. Linford, J. Lipson, and E. G. Sherwood, to be published.

[3]R. J. Commisso, R. R. Bartsch, C. A. Ekdahl, K. F. McKenna, and R. E. Siemon, Phys. Rev. Lett. 43, 442 (1979).

[4]K. F. McKenna, R. R. Bartsch, R. J. Commisso, C. Ekdahl, W. E. Quinn, and R. E. Siemon, Phys. Fluids 23, 1443 (1980).

[5]C. A. Ekdahl, Rev. Sci. Instrum. 50, 941 (1979).

[6]G. Lehner and F. Pohl, Z. Phys. 207, 104 (1967).

[7]R. C. Davidson and N. A. Krall, Nucl. Fusion 17, 1313 (1977).

[8]A. G. Sgro and C. W. Nielson, Phys. Fluids 19, 126 (1976).

[9]A. G. Sgro, Phys. Fluids 21, 1410 (1978), and 23, 1055 (1980).

[10]P. C. Liewer and N. A. Krall, Phys. Fluids 16, 1953 (1973).

[11]S. Hamasaki, N. A. Krall, C. E. Wagner, and R. N. Byrne, Phys. Fluids 20, 65 (1977).

[12]R. J. Commisso and Hans R. Griem, Phys. Rev. Lett. 36, 1038 (1976).

Structure of $p(2\times 2)$ and $c(2\times 2)$ Oxygen on Ni(100): A Surface Extended-X-Ray Absorption Fine-Structure Study

J. Stöhr and R. Jaeger

Corporate Research Science Laboratories, Exxon Research and Engineering Company, Linden, New Jersey 07036

and

T. Kendelewicz

Stanford Electronics Laboratories and Stanford Synchrotron Radiation Laboratory, Stanford University, Stanford, California 94305

(Received 28 May 1982)

In contrast to recent theoretical electronic structure calculations and analysis of electron energy-loss (ELS) spectra, surface extended-x-ray-absorption fine-structure measurements establish the local structural equivalence of $p(2\times 2)$ and $c(2\times 2)$ oxygen on Ni(100). In both cases the oxygen atoms chemisorb in the fourfold hollow site with an O-Ni bond length of 1.96 ± 0.03 Å (i.e., $d_\perp = 0.86\pm 0.07$ Å). In the light of the present results the large ELS frequency shift (14 meV) between the $p(2\times 2)$ and $c(2\times 2)$ phases remains a puzzle.

PACS numbers: 68.20.+t, 78.70.Dm

Generalized valence-bond calculations by Upton and Goddard (UG)[1] recently suggested that the chemisorption of atomic oxygen on Ni(100) leads to two distinct states. Energy minimization for oxygen in the fourfold hollow geometry and the assumption of fixed metal-atom positions resulted in respective equilibrium distances of $d_\perp = 0.88$ Å and $d_\perp = 0.26$ Å for the oxygen atom above the outermost plane of Ni atoms. Upon examining the character of the wave functions and associated charge distributions, it was concluded that the state with $d_\perp = 0.88$ Å is a *low-coverage radial state* while that with $d_\perp = 0.26$ Å is a *precursor oxide state* corresponding to higher coverage. Comparison of calculated vibrational frequencies for the two states by Rahman, Black, and Mills (RBM)[2] with those observed for $p(2\times 2)$ and $c(2\times 2)$ oxygen on Ni(100) structures by electron energy-

loss spectroscopy (ELS)[3,4] leads to a one-to-one assignment of the $d_\perp = 0.88$-Å state with the $p(2\times2)$ structure and the $d_\perp = 0.26$-Å state with the $c(2\times2)$ O on Ni(100) configuration.[1,2]

Both Upton and Goddard[1] and Rahman, Black, and Mills[2] argued that their assignment was also supported by other experimental studies. Disagreement between their $d_\perp = 0.26$-Å value and the low-energy electron-diffraction (LEED) value $d_\perp = 0.9 \pm 0.1$ Å for *both* $p(2\times2)$ (Ref. 5) and $c(2\times2)$ (Ref. 6) O on Ni(100) was attributed to a poor theoretical fit of the $c(2\times2)$ LEED data and the fact that the original LEED analysis was not carried out for distances as small as $d_\perp = 0.26$ Å.[7] In addition, x-ray photoelectron diffraction studies for the $c(2\times2)$ O on Ni(100) surface[8] were quoted as evidence that for this configuration the O atoms are in or close to the outermost plane of Ni atoms.

Here, we present a surface extended-x-ray-absorption fine-structure (SEXAFS) study of the initial oxidation stages of Ni(100). In addition to SEXAFS we carefully monitored the composition and structure of the oxygen on Ni(100) surface with increasing coverage by a combination of other techniques such as LEED, Auger, and the surface near-edge-x-ray-absorption find structure (NEXAFS) above the O K edge. From analysis of the SEXAFS phase and amplitude we conclude that the local structure around the chemisorbed O atoms is identical for the $p(2\times2)$ and $c(2\times2)$ configurations. We find a O-Ni bond length of 1.96 ± 0.03 Å and O chemisorption in the fourfold hollow site, i.e., $d_\perp = 0.86 \pm 0.07$ Å above the outermost plane of Ni atoms.

Experiments were performed on the grasshopper monochromator on beam line I-1 at the Stanford Synchrotron Radiation Laboratory. During the course of our studies two different Ni(001) crystals were employed in two different sample chambers with identical results. The crystals were cleaned by using established procedures[9,10] to exhibit a surface with less than 1% of C, O, and S. The clean and oxygen-covered surfaces were inspected by Auger and LEED. SEXAFS spectra were taken at room temperature at a base pressure of $< 2\times10^{-10}$ Torr. The crystals were exposed to oxygen whose purity was checked with a residual gas analyzer. The strongest $p(2\times2)$ pattern was observed around 1.5 L (1 L $= 10^{-6}$ Torr sec) oxygen exposure (at 1×10^{-7} Torr) and the $c(2\times2)$ pattern was most distinct around 20–30 L exposure (at 5×10^{-7} Torr) in good agreement with published results by many groups.[11,12] SEXAFS spectra of the two overlayers were recorded by partial electron yield spectroscopy with use of a two-grid detector and a retardation voltage of -350 V.[13] This resulted in a fivefold increase of the oxygen K-edge jump [~8% for $p(2\times2)$ and ~11% for $c(2\times2)$] as compared with total electron yield detection (~2%). Note that the $c(2\times2)$ oxygen overlayer corresponds to a coverage of only about 0.33 monolayer.[11] SEXAFS spectra were recorded for oxygen coverages of 1.5 L [$p(2\times2)$], 20 L [$c(2\times2)$], 90 L, 160 L, and a thermally grown thick grayish-green oxide film. We also recorded polarization-dependent NEXAFS spectra in the 1–280 L exposure range. Such spectra which are extremely sensitive to structural changes showed that no oxidelike structure was detectable below 50 L exposure. A structural analysis of the NEXAFS results will be presented elsewhere.[14]

Figure 1 compares the wave vector (k) dependent SEXAFS signals for the $p(2\times2)$ and $c(2\times2)$ O on Ni(100) overlayers recorded at an x-ray inci-

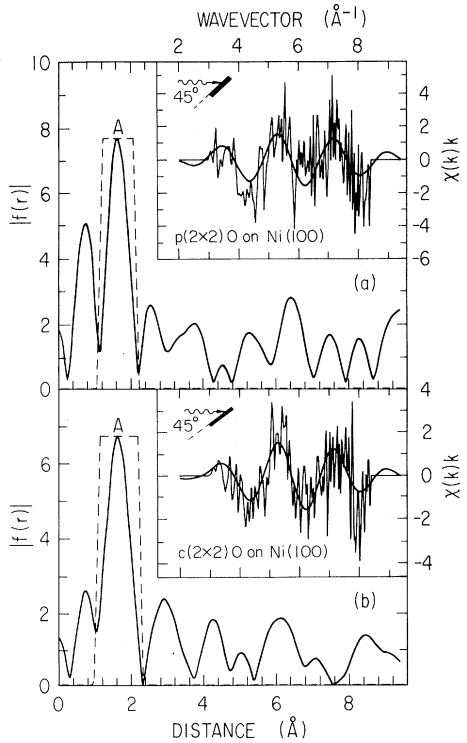

FIG. 1. (a) SEXAFS signal and absolute value of Fourier transform for 1.5 L oxygen on Ni(100) resulting in a $p(2\times2)$ LEED pattern. The SEXAFS spectrum was recorded at an x-ray angle of incidence of 45°. The smooth curve through the data corresponds to the back-transformed signal due to the O-Ni first nearest-neighbor peak A only. (b) As in (a) for 20 L oxygen on Ni(100), i.e., a $c(2\times2)$ LEED pattern.

dence angle of 45° and the corresponding Fourier transforms $|f(r)|$. The SEXAFS oscillations were normalized to the jump at the O K edge which is directly proportional to the oxygen coverage. The smooth solid line drawn through the SEXAFS data corresponds to the back-transformed signal due to peak A, only, after elimination of the other structures in $|f(r)|$ by the window function shown. Peak A corresponds to the O-Ni nearest-neighbor distance on the surface. Using a phase shift obtained from a bulk NiO standard [NiO powder, NiO single crystal, and a thermally grown thick NiO film on Ni(100) gave identical results] we determine this distance to be 1.96 ± 0.03 Å for the $p(2\times2)$ O on Ni (100) phase. For chemisorption in the fourfold hollow site this value corresponds to $d_\perp = 0.86$ Å in excellent agreement with the low-coverage radial state found by Upton and Goddard.[1]

The oxygen site for the $c(2\times2)$ O on Ni(100) phase is determined from the polarization dependence of the SEXAFS signal as previously shown for $c(2\times2)$ S on Ni(100).[10] Comparison of the polarization-dependent *amplitude ratios* for three angles of incidence unambiguously points to the fourfold hollow site as summarized in Table I. By means of the measured amplitude ratios alone we cannot distinguish between the two oxygen positions $d_\perp = 0.26$ Å proposed by Upton and Goddard[1] and $d_\perp = 0.86$ Å implied by our results for the $p(2\times2)$ phase. As listed in Table I, for both cases nearly the same amplitude ratios are expected. For $d_\perp = 0.86$ Å only the four nearest-neighbor Ni atoms in the surface plane contribute to peak A. For $d_\perp = 0.26$ Å the distance to the single Ni atom in the second substrate layer directly below the O atom becomes comparable (2.02 Å) to that to the four surface Ni atoms (1.78 Å). The sizable contribution of this fifth Ni atom at grazing x-ray incidence angles gives rise to the ambiguity found in the calculated amplitude ratios in Table I.

However, the measured O-Ni *distances* for the $c(2\times2)$ phase summarized in Table II allow an unambiguous structure determination. The O-Ni distance for $d_\perp = 0.26$ Å would be polarization dependent because of the different contributions from the surface Ni atoms and those directly underneath in the second Ni layer. No polarization dependence is observed. The measured O-Ni distance is constant and lies within 0.01 Å of that observed for the $p(2\times2)$ phase. Additional independent proof for the local equivalence of the $p(2\times2)$ and $c(2\times2)$ structures comes from comparison of the respective k-dependent SEXAFS amplitudes, recorded at 45° x-ray incidence. We obtain $A[c(2\times2)]/A[p(2\times2)] = 0.96 \pm 0.06$ indicating that the O-Ni neighbor coordination is identical. The value $d_\perp = 0.26$ Å for the $c(2\times2)$ phase would imply an amplitude ratio of 1.28 which is well outside our experimental error bar.

The present SEXAFS study unambiguously establishes for the first time the equivalence of the local oxygen chemisorption geometry for the $p(2\times2)$ and $c(2\times2)$ phases on Ni(100). Recent analysis of the $c(2\times2)$ LEED data revealed an ambiguity between configurations with $d_\perp = 0.9$ Å and $d_\perp \approx 0$ Å due to a multiple coincidence problem.[15] Photoelectron diffraction data[16] for the $c(2\times2)$ phase favored $d_\perp = 0.9$ Å but an analysis was not carried out for $d_\perp < 0.5$ Å because of computational difficulties. We do not regard the available low-energy ion scattering study[17] as an unambiguous structure determination because of its low accuracy and limited comparison with various possible surface structures. However, in retrospect the above three structural studies[15-17] are compatible with or even supportive of our re-

TABLE I. Experimental versus calculated coordination number ratios for various models of $c(2\times2)$ O on Ni(100).

X-ray incidence angle (deg)	Expt. amplitude ratio	Onefold atop	Twofold bridge[a]	Fourfold hollow with $d_\perp$(Å) = 0.26[b]	0.86[c]
90/20	2.1 ± 0.8	0	0.4	1.7	1.9
90/45	1.2 ± 0.4	0	0.5	1.3	1.4
45/20	1.8 ± 0.5	0.6	0.7	1.3	1.4

[a] Fixed Ni positions and $R_{O-Ni} = 1.96$ Å.

[b] $R_{O-Ni} = 1.78$ Å to four surface Ni atoms and $R_{O-Ni} = 2.02$ Å to one Ni atom in the second Ni layer.

[c] $R_{O-Ni} = 1.96$ Å to four surface Ni atoms.

TABLE II. Experimental versus calculated O-Ni neighbor distances in the fourfold hollow site as a function of $d_\perp$.

LEED pattern	X-ray incidence angle (deg)	Expt. O-Ni distance (Å)	Average calculated O-Ni distance (Å) for $d_\perp$(Å) = 0 [a]	0.26 [b]	0.86 [c]
$p(2\times2)$	45	1.96 ± 0.03	1.76	1.85	1.96
$c(2\times2)$	90	1.95 ± 0.03	1.76	1.78	1.96
$c(2\times2)$	45	1.96 ± 0.03	1.76	1.85	1.96
$c(2\times2)$	20	1.95 ± 0.03	1.76	1.95	1.96

[a]Each O is surrounded by 5 Ni atoms at 1.76 Å.

[b]Each O is surrounded by 4 Ni atoms at 1.78 Å and one Ni atom directly underneath at 2.02 Å.

[c]Each O is surrounded by 4 Ni atoms at 1.96 Å. The Ni atom directly below the O atom by 2.62 Å does not contribute to the first nearest-neighbor peak.

sults. Of all available structural studies only the azimuthal-photoelectron-diffraction data of Petersson *et al.*,[8] which were quoted by Upton and Goddard[1] and Rahman, Black, and Mills[2] in support of their model, appear to be contradictory. Here we have to recall that the SEXAFS signal is dominated by the *majority* species on the surface while azimuthal-photoelectron diffraction at high electron kinetic energies may well be dominated by a *minority* species in or close to the plane of Ni surface atoms.[8] We can use the SEXAFS data to derive an upper limit for such an in-plane minority species. For a worst-case analysis we assume that a fraction of O atoms indeed occupies fourfold sites with $d_\perp = 0.26$ Å ($d_\perp = 0$ Å would yield a smaller fraction of minority sites). Our error bars for the O-Ni bond length determined at 90° x-ray incidence (Table II) would allow only up to 20% O atoms in this site if we assume that no minority species is present for the $p(2\times2)$ phase. A 20% minority fraction may indeed dominate the azimuthal-photoelectron-diffraction data.

The importance of our results lies in the fundamental disagreement with the variations in structural behavior suggested by the theoretical studies[1,2] and thus we cannot accept their assignment of the puzzling changes of the ELS frequencies[3,4] in the range between the $p(2\times2)$ and $c(2\times2)$ structures (1–30 L). We do not believe that the ELS frequency shift can be explained by a possible minority species (< 20%) which builds up with increasing oxygen coverage in the 1–30 L range. The ELS oscillator strength would have to exceed that of the majority $c(2\times2)$ species by about two orders of magnitude. Since the experimental ELS spectra[3,4] appear to be reliable a new theoretical explanation of the large frequency shift needs to be found.

We would like to thank C. Troxel, Jr., for expert technical help and T. H. Upton and P. H. Citrin for valuable discussions. This work was supported in part by the National Science Foundation under Contract No. DMR77-27489 in cooperation with the Stanford Linear Accelerator Center and the Basic Energy Division of the U. S. Department of Energy and the National Science Foundation-Materials Laboratory Program through the Center for Materials Research at Stanford University.

[1]T. H. Upton and W. A. Goddard, III, Phys. Rev. Lett. 46, 1635 (1981).

[2]T. S. Rahman, J. E. Black, and D. L. Mills, Phys. Rev. Lett. 46, 1469 (1981).

[3]S. Anderson, Solid State Commun. 20, 229 (1976), and Surf. Sci. 79, 385 (1979).

[4]H. Ibach and D. Bruchmann, Phys. Rev. Lett. 44, 36 (1980); S. Lehwald and H. Ibach, in Proceedings of the International Conference on Vibrations at Surfaces, Namur, Belgium, 1980 (to be published).

[5]M. Van Hove and S. Y. Tong, J. Vac. Sci. Technol. 12, 230 (1975).

[6]J. E. Demuth, D. W. Jepsen, and P. M. Marcus, Phys. Rev. Lett. 31, 540 (1973); P. M. Marcus, J. E. Demuth, and D. W. Jepsen, Surf. Sci. 53, 501 (1975).

[7]Discrepancies among early LEED studies have been cleared up in favor of the models derived in Refs. 5 and 6. See, for example, G. Hanke, E. Lang, K. Heinz, and K. Müller, Surf. Sci. 91, 551 (1980).

[8]L. G. Petersson, S. Kono, N. F. T. Hall, S. Goldberg, J. T. Lloyd, C. S. Fadley, and J. B. Pendry, Mater. Sci. Eng. 42, 111 (1980).

[9]J. Stöhr, K. Baberschke, R. Jaeger, R. Treichler, and S. Brennan, Phys. Rev. Lett. 47, 381 (1981).

[10]S. Brennan, J. Stöhr, and R. Jaeger, Phys. Rev. B 24, 4871 (1981).

[11]P. H. Holloway and J. B. Hudson, Surf. Sci. 43, 123 (1974); D. F. Mitchell, P. B. Sewell, and M. Cohen, Surf. Sci. 61, 355 (1976); P. R. Norton, R. L. Tapping, and J. W. Goodale, Surf. Sci. 65, 13 (1977).

[12]For a review, see, C. R. Brundle, in *Aspects of the Kinetics and Dynamics of Surface Reactions—1979*, edited by U. Landman, AIP Conference Proceedings No. 61 (American Institute of Physics, New York, 1980).

[13]J. Stöhr, R. S. Bauer, J. C. McMenamin, L. I. Johansson, and S. Brennan, J. Vac. Sci. Technol. 16, 1195 (1979).

[14]D. Norman, P. J. Durham, J. B. Pendry, J. Stöhr, and R. Jaeger, to be published.

[15]S. Y. Tong and K. H. Lau, Phys. Rev. B (to be published).

[16]D. H. Rosenblatt, J. G. Tobin, M. G. Mason, R. F. Davis, S. D. Kevan, D. A. Shirley, C. H. Li, and S. Y. Tong, Phys. Rev. B 23, 3828 (1981).

[17]H. H. Brongersma and J. B. Theeten, Surf. Sci. 54, 519 (1976).

High-Precision Specific-Heat Measurements on Normal Liquid ^{3}He

Dennis S. Greywall and Paul A. Busch
Bell Laboratories, Murray Hill, New Jersey 07974
(Received 2 April 1982)

High-precision measurements have been made of the specific heat of pure liquid ^{3}He for $8 < T < 500$ mK and for $0 < P < 32.5$ bars. Such measurements have importance because of their strong bearing on our basic understanding of both normal and superfluid ^{3}He and because they provide a valuable input towards determining an absolute temperature scale at low temperatures. The specific-heat results for $T \gtrsim 100$ mK differ significantly from all of the previous measurements on ^{3}He. Only the new data, however, satisfy several important thermodynamic checks.

PACS numbers: 67.50.Dg, 65.20.+w

The effective mass of the ^{3}He quasiparticles is one of the parameters crucially needed for a basic understanding of both normal and superfluid ^{3}He. This quantity is directly related to the low-temperature specific heat of the normal liquid, a property which has been measured in many experiments[1-7] performed over the last twenty years. The results, however, differ widely, and doubts exist, for various reasons, about the correctness of even the most recent data. In this Letter we present new calorimetric data which are an attempt to resolve this important problem. The measurements were made in the temperature range 8 to 500 mK and at seven densities corresponding to nominal sample pressures between 0 and 32.5 bars. At low temperature, the new results differ significantly from all previous measurements.

In contrast to many of the earlier experiments, our calorimeter (12 cm^3) was constructed of high-purity silver, had a relatively open design, and contained no cerium magnesium nitrate (CMN) for cooling and/or thermometry. Nineteen silver wires (1.3 mm diam) were welded to the base of the cylindrical cell and penetrated the entire sample region. Silver powder[8] was sintered around each of these wires to form 2.8-mm-diam rods. The center-to-center distance between the rods was 3.5 mm. The total surface area was 2 m^2. This amount of surface area was sufficient to reduce the thermal time constants to a manageable level at low temperature but still small enough to ensure that possible surface contributions[5] to the heat capacity would be completely negligible. The heater had a resistance of 10 kΩ and was made from Pt-W wire.

Temperature measurements below 150 mK were made with a ^{3}He melting-curve thermometer[9] attached to the outside of the cell. The thermometer held approximately 0.1 cm^3 of ^{3}He and was the principal contributor to the addendum heat capacity. This background term was carefully measured and was less than a few percent of the sample heat capacity at all temperatures. This type of thermometer was used because of its high sensitivity and fast response. Moreover, the specific-heat data are now directly related to a temperature standard: the P-T relation for ^{3}He at melting.

Above 150 mK the thermometer used was a carbon resistor in an ac bridge circuit. It was calibrated during the course of each experimental run against a germanium thermometer. The latter thermometer had been calibrated previously[9]

